JOURNAL OF Materials CHEMISTRY

Metal ion mediated mesomorphism and thin film behaviour of amphitropic tetraazaporphyrin complexes

S. Holger Eichhorn,*[a]† Duncan W. Bruce,[a] Daniel Guillon,[b] Jean-Louis Gallani,[b] Thomas Fischer,[c] Joachim Stumpe[c] and Thomas Geue[d]

[a]*Department of Chemistry, University of Exeter, Stocker Rd., Exeter, UK EX4 4QD*
[b]*Institut de Physique et Chimie des Materiaux de Strasbourg, 23 rue du Loess, 67037 Strasbourg Cedex, France*
[c]*Institute of Thin Film Technology & Microsensorics, Erieseering 42, D–10319 Berlin, Germany*
[d]*University of Potsdam, Institute of Physics, P. O. Box 601553, D-14415 Potsdam, Germany*

Received 3rd January 2001, Accepted 20th March 2001
First published as an Advance Article on the web 17th April 2001

Octa-substituted tetraazaporphyrins with amphiphilic 3,6-dioxaheptylthio and 3,6,9-trioxadecylthio chains and their metal complexes (Co(II), Ni(II), Cu(II), Zn(II)) were synthesised in order to compare their thermotropic and lyotropic mesomorphism as well as their thin film properties with related tetraazaporphyrins, phthalocyanines and triphenylenes, which have been reported previously. The Co, Ni, and Cu complexes melted into hexagonal columnar mesophases, whereas the Zn(II) complexes and the free-base porphyrins did not display mesomorphism. In fact, the zinc complexes did not crystallise on cooling, rather giving highly viscous isotropic oils at room temperature that solidified below −50 °C to glasses. This unusual behaviour may be caused by axial interactions between the zinc ion and the oxygen of the polyether groups. All 3,6,9-trioxadecylthio substituted derivatives solidified far below 0 °C giving rise to columnar hexagonal mesophases at room temperature for the Co(II), Ni(II), and Cu(II) complexes. The columnar hexagonal mesophases of the long chain derivatives spontaneously align homeotropically when sandwiched between two substrates, in contrast to the short chain analogues. Both the long chain and the short chain Co(II) complexes displayed a rather disordered hexagonal columnar packing as revealed by X-ray diffraction. Binary mixtures of the short chain derivatives with non-polar or polar organic solvents did not display additional lyotropic mesophases. However, the transition temperatures and enthalpies, as well as the texture of the hexagonal columnar mesophase were affected, assuming a solubility of the solvent in the thermotropic mesophase as shown for the Cu(II) derivative. All long chain derivatives were also soluble in water but, again, lyotropic mesomorphism was observed neither with water nor with organic solvents. The film forming properties of some derivatives were investigated by spin-coating and the Langmuir–Blodgett (LB) technique. Homogeneous films of the mesomorphic short chain copper complex were obtained by the spin-coating method. The films displayed a layer structure with edge-on orientation at ambient temperature, although they were of crystalline morphology, as shown by X-ray reflectivity measurements and polarised UV/VIS spectroscopy. Only monolayer films of short and long chain derivatives could be transferred by the LB method. Again, determination of the thickness of the monolayer by X-ray agreed with an edge-on orientation of the tetraazaporphyrins. In contrast, the extrapolated molecular areas on the water surface suggested a flat-on orientation of the macrocycle with the oligo(oxyethylene) chains being dissolved in the sub-phase.

Introduction

Porphyrazines, especially phthalocyanines, are well known components of important commercial pigments, dyes and catalysts. Over the last ten years or so, they have also shown potential in many newer technologies such as photovoltaic cells, photoconductors and semiconductors, photocatalysis, electrophotography, optical data storage, fuel cells, gas sensors and photodynamic therapy of cancer.[1] Many of these newer applications require the production of thin films, preferably of controlled supramolecular order. One promising approach to such films with improved and anisotropic physical properties, is to use liquid-crystalline porphyrazine derivatives.[2] In the case of mesogenic phthalocyanines, the best results have been obtained with derivatives containing both hydrophobic alkyl and amphiphilic oligo(oxyethylene) side chains. Films of high lamellar order were easily produced by casting an amphiphilic phthalocyanine from chloroform solution onto hydrophobic substrates.[3] In general, the introduction of oligo(oxyethylene) side chains offers a promising and simple possibility to tune the material properties of discotic mesogens and can even lead to additional mesophases.

However, only few papers have been published dealing with the influence of oligo(oxyethylene) side chains on the mesomorphic behaviour of disc-like molecules.[4–7] Both lyotropic and thermotropic columnar mesophases were found for octakis(1,4,7,10-tetraoxaundecyl)[5] and tetrakis[oligo(oxyethylene)][6] substituted phthalocyanines, whereas the hexakis(1,4,7-trioxaoctyl)triphenylene only displays aqueous lyotropic columnar mesophases.[7] The mesomorphism of the former is obviously dominated by the strong π-interactions of the large aromatic system of the phthalocyanine unit, while the mesomorphism of the latter, containing a much smaller

†*Present address*: Massachusetts Institute of Technology, 77 Massachusetts Avenue, Rm18-110, Cambridge, MA 02139, USA. sheich@mit.edu; Fax: +1 (617)627-9028; Tel: +1 (617)258-6536.

 DOI: 10.1039/b100112o

π-electron system, is dominated by the amphiphilic side chains. A systematic investigation of the influence of different metal ions on the mesomorphism of oligo(oxyethylene) substituted porphyrazines has not yet been presented, but recent papers on amphiphilic metallophthalocyanines do reveal a distinct influence of the metal ion.[8,9] It should be mentioned here that some disc-shaped molecules containing oligo(oxyethylene) side chains were synthesised in the 1970s (octopus molecules), but their mesomorphism was not investigated.[10] Further, crown ether substituted porphyrazines have been investigated for some time,[11] while the immiscibility of alkyl and oligo(oxyethylene) chains has been used to produce lamellar mesophases of annelide-type copper complexes containing both types of chains.[12]

However, the aim of this study was to investigate the thermotropic as well as lyotropic mesomorphism of the octakis(3,6-dioxaheptylthio) and octakis(3,6,9-trioxadecylthio) substituted tetraazaporphyrins and their metal complexes as mesogens containing a medium sized aromatic system.[13,14]

Experimental

Materials

All commercially available chemicals were of analytical grade; solvents were dried over molecular sieves and used without further purification. For flash chromatography Matrix Silica Si chromatography medium (60 Å 35–70 μm particle size), a product of Amicon (Witten, Germany), or RP-18 material from Merck (LiChroprep RP-18, 25–40 μm) was used. Thin layer chromatography (TLC) was carried out using Macherey-Nagel's (Düren, Germany) Polygram 0.25 mm SIL G/UV_{254} pre-coated plastic sheets.

Equipment and measurements

For analysis the following instruments were used: UV/VIS-absorption spectra by a Perkin Elmer Lambda 9 as well as a specially equipped Perkin Elmer 119 and a microscope spectrometer (Photomikroskop III from Carl Zeiss) for polarized spectroscopy; FT-IR spectra by a Bio-Rad Digilab FT-IR FTS7 instrument; ^{1}H- and ^{13}C-NMR spectra by a Bruker WH 360 or 300 spectrometer (using the deuterium signal of the solvent as the lock and tetramethylsilane as internal standard). The HPLC chromatograms were recorded with a Merck-Hitachi-System (L-3000 Photo Diode Array Detector, L-6200A Intelligent Pump, T-6300 Column Thermostat, AS 2000A Autosampler). A Merck LiChrospher Si-60 (5 μm) with 250 mm length and 4 mm inner diameter was used as the column. The DSC measurements were carried out on a Polymer Laboratories DSC with an Auto-Cool-System and a Perkin Elmer DSC 7. A polarizing microscope (Leitz, Wetzlar) with hot stage was used for optical investigations. Powder X-ray diffraction patterns were recorded at 40 °C using a Guinier-type camera with bent quartz monochromator ($CuK\alpha_1$ radiation, $\lambda = 1.54$ Å), an INSTEC hot-stage (±0.01 °C) and an INEL curved position-sensitive gas detector. Samples were housed in sealed Lindemann glass capillaries. The mixtures with different solvents were placed between two glass slides and sealed with an epoxy glass glue for the optical investigation. DSC measurements were carried out on two samples (2.44 mg and 2.89 mg of **Cu52** were combined with 9.01 mg ethylene glycol and 8.21 mg decane, respectively) which were placed in sealed aluminium pans (PE No. 0319-0218, max. recommended pressure is 24 atm).

X-Ray reflectivity and diffuse scattering measurements of spin-coated thin film samples were carried out on a STOE θ–θ-diffractometer using a conventional angular-dispersive setup in $\theta_i = \theta_f$ mode at $\lambda = 1.54$ Å ($CuK\alpha$ radiation while $CuK\beta$ line was suppressed using a Ni filter). The scattered intensity was recorded with a conventional NaI scintillation counter. The source and detector apertures were usually set to parameters (several mm in the *y*-; 10 to 30 μm in the *z*-direction) where no additional scattering from the edges of the apertures could be detected which would have major influences on the symmetry of the primary beam profile so that we were able to separate influences due to the geometry from the experimental set-up and of the sample from each other. The sample was adjusted in the midpoint of the goniometer set-up in order to avoid geometric correction. The measured reflectivity curves were recorded in two ranges, first next to the absorption edge of material and substrate with an external steel filter placed in front of the detector window in order to avoid radiation damage in the detector. The small angle region was recorded without any filter.

Langmuir and Langmuir–Blodgett film preparations were performed on a KSV5000 system. Typically, 50 μL of a *ca.* 2 mg ml^{-1} concentrated solution in chloroform were spread on the water surface. We gave the Langmuir films 20 minutes to stabilise before starting the compression. The presented isotherms were recorded with a compression speed of about 18 $Å^2$ $molecule^{-1}$ $minute^{-1}$. However, the observed behaviour showed almost no dependence on the compression speed. Ultra-pure water (Millipore system) was used as a sub-phase and the temperature was set to 20 (±0.5) °C for the reported measurements. Generally, isotherms showed little dependence on the temperature between 10 and 50 degrees.

Polished silicon ⟨111⟩ substrates were used for the preparation of Langmuir–Blodgett films. They were cleaned prior to transfer using the following procedure: the plates were immersed in an ultrasonic bath with an oxidising mixture H_2SO_4–H_2O_2 (1 : 1), then rinsed at least 15 times with ultra-pure water. The grazing incidence X-ray studies of LB films were performed on an X'PERT-MPD device from Philips, equipped with a Nickel beta filter, a programmable divergence slit (1/32°), a parallel plate collimator, a flat Ge monochromator and a proportional Xe detector. $CuK\alpha$ line (wavelength = 0.1542 nm) was used. All measurements were recorded immediately after the LB film transfer.

Synthesis

Disodium 1,2-dicyanoethylene-1,2-dithiolate; 1. The compound was prepared by the method of Davison and Holm.[15] The UV/VIS and FT-IR spectra agreed with the reported spectra in the literature.

1,3,6,9-Tetraoxaundecyl tosylate. The compound was prepared by the method of Lee and Oh.[16] The NMR and FT-IR spectra agreed with the reported spectra in the literature.

1,2-Dicyano-1,2-bis(3,6-dioxaheptylthio)ethylene and 1,2-dicyano-1,2-bis(3,6,9-trioxadecylthio)ethylene; 2 and 3. To a vigorously stirred suspension of **1** (1.86 g, 10 mmol) in propan-1-ol (20 mL) a solution of 2-(2-methoxyethoxy)ethyl bromide (3.48 g, 19 mmol) and sodium iodide (150 mg, 1 mmol) or a solution of 1,3,6,9-tetraoxaundecyl tosylate (6.05 g, 19 mmol) in propan-1-ol (10 ml) was added dropwise. After 24 h the solvent was evaporated under vacuum and the brown, oily residue was extracted with dry, hot *tert*-butyl methyl ether until colourless. After evaporation of the ether under vacuum, the oil was stirred at 80 °C and 5 Pa until the weight was constant to afford a reddish-brown, highly viscous product. Further purification for analytically pure samples was achieved by flash chromatography on alumina using diethyl ether–DCM mixtures as solvent (2 : 1 for **2** and 9 : 1 for **3**).

2 (2.44 g, 70%), UV/VIS: λ_{max} (EtOH) 218 nm (5200 ε/dm^3 mol^{-1} cm^{-1}), 273 (4200), 330 shoulder, 339 (13000); IR: ν_{max}/cm^{-1} 2926, 2878 and 2828 (CH), 2212 (CN), 1654br (C=C); ^{1}H-NMR: δ (360 MHz; $CDCl_3$) 3.74 (4 H, t), 3.62 (4 H,

m), 3.52 (4 H, m), 3.37 (6 H, s), 3.31 (4 H, t, SCH_2); ^{13}C-NMR: δ (360 MHz; $CDCl_3$) 121.17 (C=C), 112.11 (C≡N), 71.73, 70.52, 69.46 (all OCH_2), 59.03 (CH_3), 34.67 (SCH_2); MS: *m/z* (FAB(−), glycerin) 346 (M^-, 1.4%), 243 ($M-(C_2H_4O)_2CH_3)^-$, 100%), 140 ($M-2\{(C_2H_4O)_2CH_3)^-$, 36%).

3 (3.43 g, 79%), UV/VIS: λ_{max} (EtOH) as for **2**; IR: ν_{max}/cm^{-1} as for **2**; ^{1}H-NMR: δ (300 MHz; $CDCl_3$) 3.77 (4 H, t), 3.68 to 3.54 (16 H, m), 3.38 (6 H, s), 3.33 (4 H, t, SCH_2); ^{13}C-NMR: δ (300 MHz; $CDCl_3$) 121.59 (C=C), 112.58 (C≡N), 72.26, 70.99, 70.90, 69.63, 69.02 (all OCH_2), 59.39 (CH_3), 34.67 (SCH_2); MS: *m/z* (FAB(+), mNBA) 435 (M^+, 100%).

2,3,7,8,12,13,17,18-Octakis(3,6-dioxaheptylthio)-5,10,15,20-tetraazaporphyrin and 2,3,7,8,12,13,17,18-octakis(3,6,9-trioxadecylthio)-5,10,15,20-tetraazaporphyrin; H52 and H73. Mg powder (48.6 mg, 2 mmol) was refluxed overnight in dry 50 ml propan-1-ol. **2** (3.43 g, 10 mmol) or **3** (4.35 g, 10 mmol) was added, and the stirred suspensions were again heated to reflux for 36 h. The resulting blue suspension was filtered, and the residue was washed with propan-1-ol. The solvent from the collected extracts was evaporated and the residues were stirred in 50 ml hot (80 °C) acetic acid for 30 to 60 min. The progress of demetallation was monitored by VIS spectroscopy. The purple solutions were added to 200 ml distilled water to give a fine precipitate for **H52** but **H73** did not phase separate and was extracted with *tert*-butyl methyl ether. **H52** was filtered off, washed with pure water and then freeze-dried. The ether solution of **H73** was extracted with pure water, dried over $MgSO_4$, and evaporated. A very crude oil was obtained and filtered through silica using toluene–ethyl acetate 1 : 1 as solvent. Both products were used for the following metallations without further purification. For analytical measurements, however, a higher purity was achieved by column chromatography on RP-18 (Biotage, flash 40) using methanol (**H52**) or methanol–water 9 : 1 (**H73**) as eluents.

H52 (1.89 g, 55%), UV/VIS: λ_{max} (THF) 356 nm (51200 ε/$dm^3\,mol^{-1}\,cm^{-1}$), 504 (22200), 636 (29500), 708 (38500); IR: ν_{max}/cm^{-1} 2929, 2877 and 2824 (CH), 1111 (COC), 1028; ^{1}H-NMR: δ (360 MHz; $CDCl_3$) 4.29 (16 H, t, SCH_2), 3.98 (16 H, t), 3.62 (16 H, m), 3.44 (16 H, m), 3.25 (24 H, s), −1.14 (2 H, s); ^{13}C-NMR: δ (360 MHz; $CDCl_3$) 152.9 ($CN_{arom.}$), 140.0 ($C{=}C_{arom.}$), 71.7, 71.0, 70.2, 58.8 (CH_3), 34.5 (SCH_2); MS: *m/z* (DCI(−), NH_3) 1386 (M^-, 100%).

H73 (1.83 g, 42%), UV/VIS: λ_{max} (THF) as for **H52**; IR: ν_{max}/cm^{-1} as for **H52**; ^{1}H-NMR: δ (500 MHz; $CDCl_3$) 4.29 (16 H, t, SCH_2), 3.98 (16 H, t), 3.65 (16 H, m), 3.57 (16 H, m), 3.52 (16 H, m), 3.43 (16 H, m), 3.28 (24 H, s), −1.20 (2 H, s); ^{13}C-NMR: δ (500 MHz; $CDCl_3$) 153.8 ($CN_{arom.}$), 141.0 ($C{=}C_{arom.}$), 72.5, 71.6, 71.2, 71.1, 71.0, 59.7 (CH_3), 35.2 (SCH_2); MS: *m/z* (FAB(+), mNBA) 1739.6 ($M+H^+$, 24%), 1619.3 ($M+H-((C_2H_4O)_2CH_3)^+$, 100%). Exact mass 1738.6391 ± 0.0051, calculated 1738.6337.

2,3,7,8,12,13,17,18-Octakis(3,6-dioxaheptylthio)-5,10,15,20-tetraazaporphyrinato-cobalt, -nickel, -copper or -zinc Co52, Ni52, Cu52, Zn52. H52 (500 mg, 0.36 mmol) and the corresponding metal(II) diacetate (0.5 mmol) were refluxed in 50 ml methanol for about 2 h (copper) to 8 h (nickel). The metallations were monitored by VIS spectroscopy and stopped when the absorption bands of the free ligand had fully disappeared. The cold suspensions were added to 100 ml 5% aqueous NH_4Cl solution. The blue precipitates of **Ni52** and **Cu52** were filtered and washed with hot distilled water, while the oily phases of **Co52** and **Zn52** were extracted with *tert*-butyl methyl ether, washed with pure water, dried over $MgSO_4$ and then evaporated. All products were further purified as described for **H52** by column chromatography first on silica and finally on RP-18.

Ni52 (473 mg, 91%), UV/VIS: λ_{max} (THF) 326 nm (44300 ε/$dm^3\,mol^{-1}\,cm^{-1}$), 482 (18100), 661 (41900); IR: ν_{max}/cm^{-1} as for **H52**; ^{1}H-NMR: δ (500 MHz; $CDCl_3$) 4.21 (16 H, t, SCH_2), 3.94 (16 H, t), 3.61 (16 H, m), 3.46 (16 H, m), 3.27 (24 H, s); ^{13}C-NMR: δ (500 MHz; $CDCl_3$) 149.7 ($CN_{arom.}$), 142.4 ($C{=}C_{arom.}$), 72.5, 71.7, 71.1 (all OCH_2), 59.7 (CH_3), 35.3 (SCH_2); MS: *m/z* (FAB(+), mNBA) 1444 ($M+H^+$, 100%). Exact mass 1442.3482 ± 0.0042, calculated 1442.3437.

Co52 (458 mg, 88%), UV/VIS: λ_{max} (THF) 355 nm (48500 ε/$dm^3\,mol^{-1}\,cm^{-1}$), 455 (12100), 643 (46300); IR: ν_{max}/cm^{-1} as for **H52**; MS: *m/z* (FAB(+), mNBA) 1444 ($M+H^+$, 100%). Exact mass 1443.3394 ± 0.0042, calculated 1443.3416.

Cu52 (495 mg, 95%), UV/VIS: λ_{max} (THF) 352 nm (41900 ε/$dm^3\,mol^{-1}\,cm^{-1}$), 496 (15500), 664 (45100); IR: ν_{max}/cm^{-1} as for **H52**; MS: *m/z* (DCI^-, NH_3) 1449 (M^-, 100%). Elemental analysis, found: C, 46.87; H, 6.20; N, 7.65; O, 17.50; S, 17.37%. $C_{56}H_{88}N_8O_{16}S_8Cu$ requires C, 46.41; H, 6.12; N, 7.73; O, 17.66; S, 17.70%.

Zn52 (449 mg, 86%), UV/VIS: λ_{max} (THF) 375 nm (64400 ε/$dm^3\,mol^{-1}\,cm^{-1}$), 672 (69800); IR: ν_{max}/cm^{-1} as for **H52**; ^{1}H-NMR: δ (360 MHz; $CDCl_3$) 4.24 (16 H, t, SCH_2), 3.94 (16 H, t), 3.51 (16 H, m), 3.32 (16 H, m), 3.11 (24 H, s); ^{13}C-NMR: δ (360 MHz; $CDCl_3$) 156.5 ($CN_{arom.}$), 140.6 ($C{=}C_{arom.}$), 71.6, 71.2, 69.9, 58.7 (CH_3), 34.4 (SCH_2); MS: *m/z* (DCI^-, NH_3) 1450 (M^-, 100%). Elemental analysis, found: C, 46.41; H, 6.15; N, 7.80; S, 17.73%. $C_{56}H_{88}N_8O_{16}S_8Zn$ requires C, 46.35; H, 6.11; N, 7.72; S, 17.67%.

2,3,7,8,12,13,17,18-Octakis(3,6,9-trioxadecylthio)-5,10,15,20-tetraazaporphyrinato-cobalt, -nickel, -copper or -zinc Co73, Ni73, Cu73, Zn73. H73 (200 mg, 0.11 mmol) and the corresponding metal(II) diacetate (0.3 mmol) were refluxed in 50 ml methanol for about 2 h (copper) to 8 h (nickel). The metallations were monitored by VIS spectroscopy and stopped when the absorption bands of the free ligand had fully disappeared. The cold suspensions were added to 100 ml 5% aqueous NH_4Cl solution and the blue products were extracted with *tert*-butyl methyl ether, washed with pure water, dried over $MgSO_4$, and then evaporated. All products were further purified as described for **H73** by column chromatography first on silica and finally on RP-18.

Co73 (148 mg, 75%), λ_{max} (THF) 354 nm (49700 ε/$dm^3\,mol^{-1}\,cm^{-1}$), 456 (12200), 645 (47400); ν_{max}/cm^{-1} as for **H73**; MS: *m/z* (FAB(+), mNBA) 1797 ($M+H^+$, 100%), 1677 ($M+H-(C_5H_{12}O_3)^+$, 37%). Exact mass 1795.5467 ± 0.0051, calculated 1795.5513.

Ni73 (164 mg, 83%), UV/VIS: λ_{max} (THF) 327 nm (44900 ε/$dm^3\,mol^{-1}\,cm^{-1}$), 483 (18900), 661 (42600); IR: ν_{max}/cm^{-1} as for **H73**; ^{1}H-NMR: δ (500 MHz; $CDCl_3$) 4.19 (16 H, t, SCH_2), 3.94 (16 H, t), 3.64 (16 H, t), 3.57 (16 H, t), 3.53 (16 H, t), 3.44 (16 H, t), 3.28 (24 H, s); ^{13}C-NMR: δ (500 MHz; $CDCl_3$) 149.7 ($CN_{arom.}$), 142.5 ($C{=}C_{arom.}$), 72.5, 71.6, 71.2, 71.2, 71.1 (all OCH_2), 59.7 (CH_3), 35.4 (SCH_2); MS: *m/z* (FAB(+), mNBA) 1796 ($M+H^+$, 100%), 1676 ($M+H-(C_5H_{12}O_3)^+$, 48%). Exact mass 1794.5502 ± 0.0051, calculated 1794.5535.

Cu73 (174 mg, 88%), UV/VIS: λ_{max} (THF) 351 nm (42800 ε/$dm^3\,mol^{-1}\,cm^{-1}$), 496 (15900), 662 (46200); IR: ν_{max}/cm^{-1} as for **H73**; MS: *m/z* (FAB(+), mNBA) 1801 ($M+H^+$, 100%), 1681 ($M+H-(C_5H_{12}O_3)^+$, 32%). Exact mass 1799.5426 ± 0.0051, calculated 1799.5477.

Zn73 (155 mg, 78%), UV/VIS: λ_{max} (THF) 372 nm (67900 ε/$dm^3\,mol^{-1}\,cm^{-1}$), 668 (68700); IR: ν_{max}/cm^{-1} as for **H73**; ^{1}H-NMR: δ (500 MHz; $CDCl_3$) 4.27 (16 H, m, SCH_2), 3.91 (16 H, m), 3.50 (16 H, m), 3.41 (16 H, m), 3.30 (16 H, m), 3.23 (16 H, m), 2.88 (24 H, s); ^{13}C-NMR: δ (500 MHz; $CDCl_3$) 157.3 ($CN_{arom.}$), 141.6 ($C{=}C_{arom.}$), 72.1, 71.2, 71.0, 70.7, 70.0 (all OCH_2), 59.2 (CH_3), 35.2 (SCH_2); MS: *m/z* (FAB(+), mNBA) 1802 ($M+H^+$, 36%), 1682 ($M+H-(C_5H_{12}O_3)^+$, 100%). Exact mass 1800.5533 ± 0.0054, calculated 1800.5472.

Results and discussion

Synthesis and characterisation

The readily available 1,2-dicyanoethylene-1,2-dithiolate, **1**, was employed as starting material for the preparation of the title compounds. Compound **1** was reacted with 3,6-dioxaheptyl bromide or 1,3,6,9-tetraoxaundecyl tosylate after a modification of the procedure of Schramm and Hoffman[17,18] to give 1,2-dicyano-1,2-bis(3,6-dioxaheptylthio)ethylene (**2**) or 1,2-dicyano-1,2-bis(3,6,9-trioxadecylthio)ethylene (**3**) in moderate yields of around 70%. The dinitriles, **2** and **3**, were then cyclotetramerized in a mixture of magnesium propanolate and propan-1-ol to give octakis(3,6-dioxaheptylthio)tetraazaporphyrinatomagnesium and octakis(3,6,9-trioxadecylthio)tetraazaporphyrinatomagnesium, respectively. The crude magnesium complexes were directly converted into the metal-free tetraazaporphyrins, **H52**, and, **H73**, respectively, in around 55% yield overall, by heating the magnesium complexes in ethanoic acid at 80 °C for about 20 min (Scheme 1).[19]

Azaporphyrins **H52** and **H73** can be metallated by heating with metal salts in methanol as is shown in this work for the reactions with cobalt(II), nickel(II), copper(II) and zinc(II) acetate, with almost quantitative formation of the corresponding metal complexes **Co52** to **Zn73**, respectively. A yield of about 90% was obtained for the short chain derivatives and of about 80% for the long chain derivatives. The losses are due to the elaborate purification by chromatography first on silica and finally on RP-18. **Co52** and **Co73** were purified under exclusion of oxygen and light to minimise decomposition and oxidation to Co(III).

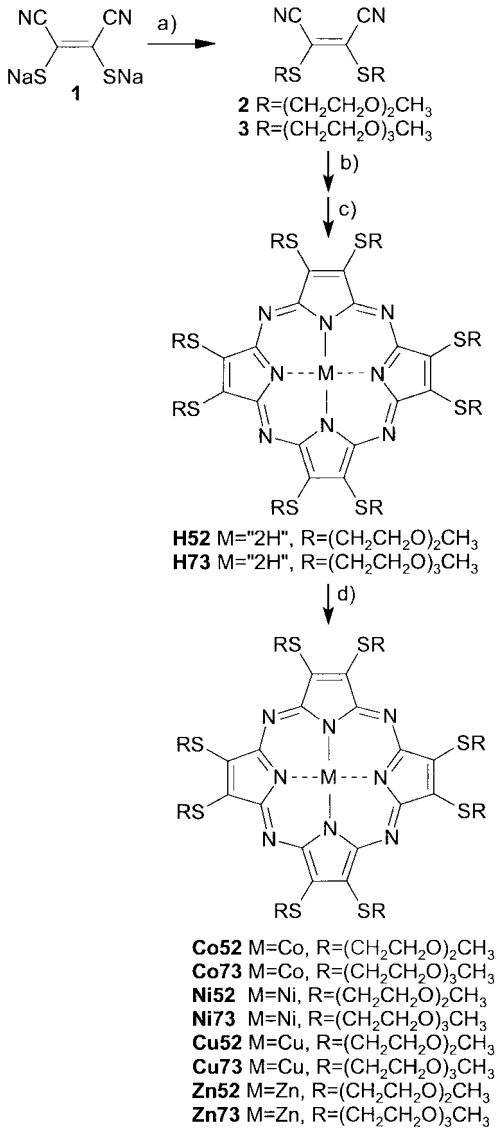

Scheme 1 Synthetic pathway to the oligo(oxyethylene) substituted tetraazaporphyrins. *Reagents and conditions*: a.) $Br(C_2H_4O)_2CH_3$ or $TsO(C_2H_4O)_3CH_3$, KI, propan-1-ol. b.) Mg propanolate, propan-1-ol, reflux. c.) acetic acid, 80 °C, 20 min. d.) metal(II)Ac_2, methanol, reflux.

The identity and purity of all compounds were determined by UV/VIS (see Table 3), IR and NMR spectroscopy, mass spectrometry and chromatography (see Experimental). The ^{1}H-NMR signals of the cobalt and copper compounds were much broadened due to the presence of the paramagnetic metal ions. Compounds **Zn52** and **Cu52** were also characterised by elemental analysis and additional high resolution MS data were collected for the long chain derivatives. A purity of the tetraazaporphyrins of $\geqslant$99% was determined by normal and reverse phase chromatography (HPLC and TLC).

Thermotropic mesomorphism

Investigations by polarising optical microscopy indicated the formation of hexagonal columnar mesophases by the Co, Ni, and Cu complexes, whereas the free-base and Zn derivatives did not display mesomorphism. The mesomorphic 3,6,9-trioxadecylthio substituted complexes spontaneously aligned homeotropically when sandwiched between treated or untreated glass plates and displayed the typical pseudo-isotropic dendritic hexagon texture of a Col_h mesophase

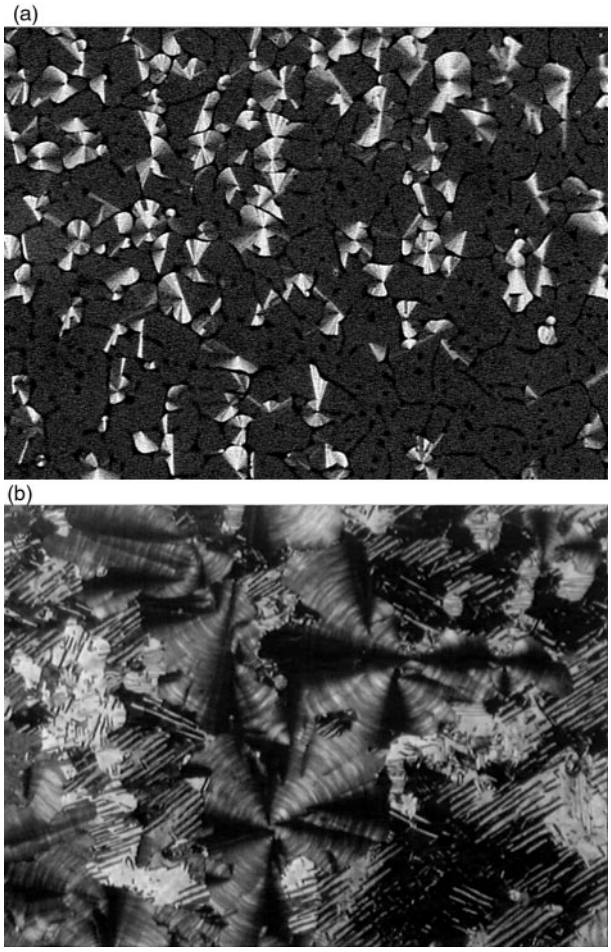

Fig. 1 a): Photomicrograph of a focal-conic-like texture of **Ni73** containing big pseudo-isotropic areas obtained on cooling from the isotropic melt (2 μm, 200×, no analyser, 22 °C); b): a focal-conic-like texture growing into a mosaic-like texture of **Cu52** on cooling (92×, crossed polarizers, 100 °C).

Table 1 Transition temperatures and enthalpies of the 2nd heating run and the 1st cooling run [ ] determined by DSC (10 °C min^{-1})

	T/°C (ΔH/kJ mol^{-1})		
Comp.	K↔Col	Col↔Col$_h$	Col$_h$↔I
H52	55 (58.0) [26 (−57.7)]		
Co52	−5.5 (32.5) [−20.9 (−30.7)]		170.4 (1.6) [169.4 (−2.6)]
Ni52	44.2 (25.6) [24.6 (−18.8)]	[34.8 (−0.8), 54.8 (−0.3)]	115.3 (3.2) [113.7 (−5.3)]
Cu52	61 (51.5) [38 (−49.9)]		152 (9.8) [148 (−14.4)]
Zn52	−51 (T_g)		
H73	−75.8 (T_g), −53.1 (−4.3)[a], −33.7 (2.4) [−79.9 (T_g)]		
Co73	−76.5 (T_g) [−77.1 (T_g)]		64.2 (1.2) [49.6 (−1.4)]
Ni73	−33.5 (−9.6)[a], −11.6 (21.3) [−48 (−11.6)][b]	10.3 (0.5) [8.6 (−0.6)]	40.2 (5.7) [39.8 (−6.8)]
Cu73	−16.0 (49.8) [−28.5 (−46.6)]		56.2 (3.9) [53.4 (−6.8)]
Zn73	−63.8 (T_g) [−64.4 (T_g)]		

[a]Cold crystallisation on heating. [b]Very broad transition including type of glass transition at about −80 °C.

(Fig. 1a).[20] In contrast, the mesomorphic short chain complexes did not spontaneously align homeotropically and rather displayed pseudo-focal-conic textures. **Cu52** also gave a mosaic-like texture when sandwiched between untreated glass slides (*ca.* 2 μm thick layer) and cooled at 0.1 min^{-1} from the isotropic melt. Annealing of the thin layer at 100 °C for several hours again led to a radial banded pseudo-focal-conic texture (Fig. 1b). This new texture, once fully developed, did not show any optical changes on cooling. Both the mosaic-like and the pseudo-focal-conic texture[21] have already been reported for columnar mesophases.

Phase transition temperatures and enthalpies determined by differential scanning calorimetry (DSC) are presented in Table 1. Both the long and the short chain series show a similar metal ion dependence. Cobalt as central metal ion gave the widest mesophase temperature ranges (175 °C for **Co52**) followed by copper and then nickel. Nickel, however, promoted a certain polymesomorphism and additional peaks of very small transition enthalpy were found between the melting and the clearing transitions. For **Ni52**, the two additional transitions on cooling were also confirmed by minor changes of the microscopic texture. They presumably represent transitions to higher ordered biaxial columnar mesophases but were not investigated in greater detail.

The metal-free and the zinc derivatives are non-mesomorphic and the latter complexes did not even crystallise. Instead, glass transitions were found for **Zn52** and **Zn73** at

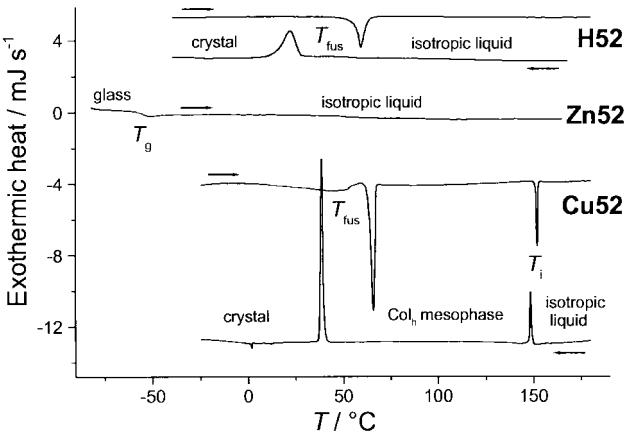

Fig. 2 DSC curves of **H52** and **Zn52** (10 °C min^{-1}) and **Cu52** (5 °C min^{-1}).

−51 °C and −64 °C, respectively (Fig. 2).[22] A higher tendency to freeze in as glass was also found for all long chain derivatives and is particularly true for samples containing small amounts of water.

Powder X-ray diffraction measurements confirmed the existence of a disordered hexagonal columnar mesophase (Col$_{hd}$) for the nickel and the copper derivatives (Table 2). Three characteristic Bragg diffraction peaks in the low angle region (ratio 1, $\sqrt{3}$, $\sqrt{4}$) and a diffuse signal in the wide angle region due to the liquid-like state of the terminal chains were found for the nickel and the copper complexes. The intercolumnar distances of about 20.5 Å and 23.3 Å derived from the diffraction data agreed with the calculated molecular dimensions assuming a liquid like conformation of the side chains. **Cu52** was studied in more detail and the two-dimensional hexagonal parameter was found to vary from 17.75 Å (60 °C) to 18.00 Å (150 °C), corresponding to a distance between neighbouring columns varying from 20.5 Å to 20.8 Å. In contrast, both cobalt derivatives displayed only one broad peak in the small angle region and calculated values of the spacing were slightly smaller than for the analogous nickel or copper compounds (Fig. 3). The appearance of the diffraction patterns and the small clearing enthalpy were more reminiscent of a nematic type phase but the microscopic texture analysis verified the phase assignment. However, the cobalt complexes certainly display a hexagonal columnar mesophase with disturbed long-range positional order.

The non-mesomorphic behaviour of **H52** and **H73** was expected, since the octakis(alkylthio)tetraazaporphyrins of comparable chain length are not mesomorphic in contrast to their cobalt, nickel, copper and zinc derivatives.[13] However, the totally different behaviour of **Zn52** and **Zn73** was surprising and may be explained by a higher coordination number of the zinc ion in the macrocycle, due to inter- or intra-molecular axial binding between the zinc ion and the oxygen of the ether groups. An axial interaction of the oxygen ether with the cobalt ions of **Co52** and **Co73** might also account for the disturbed columnar packing.[23] Porphyrin and azaporphyrin ligands

Table 2 X-Ray diffraction data of the mesomorphic cobalt, nickel and copper complexes

Compound	d/Å (hkl)	Intercolumnar spacing/Å	T/°C
Co52[a]	17.28 (100)[a]	19.9	71
Ni52	17.87 (100), 10.45 (110), 9.06 (200), 4.4 (halo)	20.6	68
Cu52	17.75 (100), 10.23 (110), 8.90 (200), 4.3 (halo)	20.5	60
Co73[a]	19.06 (100)[a]	22.0	30
Ni73	20.09 (100), 11.81 (110), 10.14 (200), 4.5 (broad halo)	23.2	26
Cu73	20.09 (100), 11.81 (110), 10.14 (200), 4.5 (broad halo)	23.2	27

[a]The (100) reflection has an exponentially decaying tail towards higher angles that smoothly incorporated the side chain halo at about 4.5 Å as can be seen from Fig. 3.

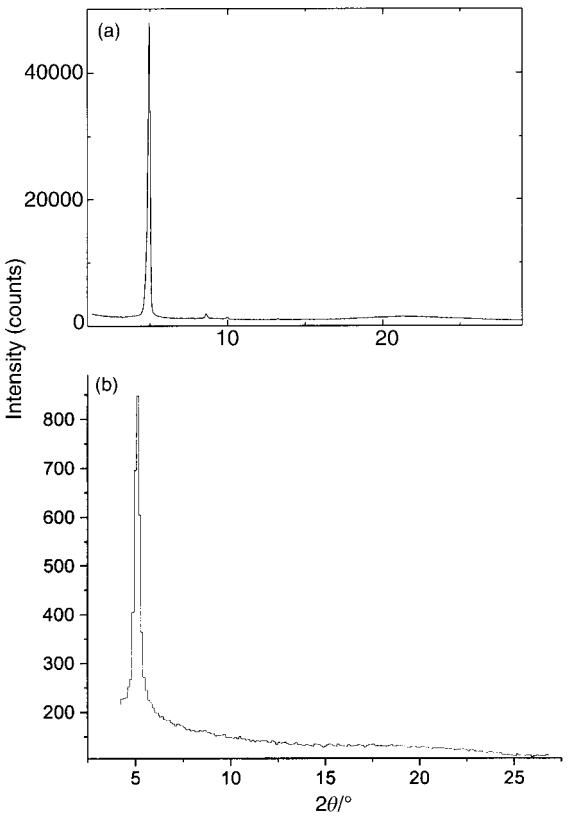

Fig. 3 X-Ray diffraction patterns of **Cu52** (a) and **Co52** (b) at 60 °C and 71 °C, respectively.

containing ions such as Mg(II), Mn(II), Co(II) and Zn(II) are well known for their high affinity to O and N containing donor ligands whereas Ni and Cu only weakly bind N-donor ligands in the axial position.[24] However, heteroatoms directly bound to the aromatic macrocycle apparently do not function as strong enough ligands[25] and do not obstruct the face to face packing in the columnar mesophase. Other evidence supporting this hypothesis is given by the non-crystallinity of octa-substituted magnesium(II)- and zinc(II)-tetraazaporphyrins containing alkylthio chains with terminal hydroxy groups.[26] However, this particular metal ion effect is less pronounced in related phthalocyanines[27] since the cofacial interaction energy is much higher due to the increased size of the aromatic system.

The relative differences in transition temperatures and enthalpies of the cobalt, nickel and copper derivatives are similar to what was found for the parent octakis(alkylthio)-tetraazaporphyrinato metal complexes.[13] However, the absolute values for the 3,6-dioxadecylthio and the 3,6,9-trioxadecylthio substituted derivatives are smaller when compared to alkyl substituted derivatives of comparable chain length. This seems to be a general trend, as a similar behaviour was found for octa-substituted phthalocyanines comparing derivatives containing oligo(ethyleneoxy) side chains with alkyloxy substituted derivatives of similar chain length.[5b]

Solvent containing mesophases

Sealed contact samples of all presented tetraazaporphyrins with non-polar solvents (hexadecane, decane, CS_2), polar aprotic (dibutyl ether, 1,2-dimethoxyethane) and with polar protic solvents (water, methanol, mixtures of water and methanol, ethylene glycol) were studied for lyotropic mesomorphism. At 30 °C all compounds gave isotropic solutions in CS_2, dibutyl ether, 1,2-dimethoxyethane, and methanol, while they were insoluble in hexadecane and decane. Water and ethylene glycol only dissolved the derivatives containing the long 3,6,9-trioxadecylthio side chains at 30 °C. Elevated temperatures led to solubility in all of the before mentioned solvents, but lyotropic mesomorphism was not observed in any of the mixtures. Particularly surprising was the missing lyotropic mesomorphism of the long chain derivatives in water solution. UV/VIS spectroscopy did reveal some H-aggregation, a blue shift of the Q-bands (Table 3), but it did not result in the formation of an additional lyotropic mesophase with increased concentration of the porphyrazine. In contrast, octakis(1,4,7,10-tetraoxaundecyl)phthalocyanines[5] and hexakis(1,4,7-trioxaoctyl)triphenylene[6] have been found to display lyotropic mesomorphism over a wide concentration range.

However, the contact samples also showed that small amounts of solvent did dissolve in the thermotropic mesophases of the cobalt, nickel, and copper complexes without fully disturbing the mesophase. That was particularly obvious for mixtures of **Cu52** with hexadecane, decane and ethylene glycol. The transition temperatures of the thermotropic mesophase were drastically reduced by up to 50 °C and the textures changed although the separated solvent phase was still uncoloured, suggesting no solubility of **Cu52** in the solvent. On cooling from the isotropic phase, fern-like textures, also typical for hexagonal columnar mesophases,[28] were obtained in addition to the aforementioned textures. Two phase mixtures of **Cu52** with decane (74%$_{mass}$) and ethylene glycol (79%$_{mass}$) were investigated by DSC in order to confirm the microscopic observations and to determine transition enthalpies. For both the decane and the ethylene glycol mixtures clearing temperatures were reduced to 106 and 108 °C whereas the enthalpies were increased to 11.7 and 13.3 kJ mol^{-1}, respectively. The melting temperature, however, was reduced only by ethylene glycol showing a melting transition of 50 °C and a recrystallisation at 26 °C (instead of 61 °C and 38 °C for the pure **Cu52**, respectively), but the enthalpies were reduced for both the decane ($\Delta H = 47.6$ kJ mol^{-1}) and the ethylene glycol ($\Delta H = 52.6$ kJ mol^{-1}) mixtures. This behaviour can be explained with small amounts of solvent being dissolved in

Table 3 UV/Vis absorption maxima and molar extinction coefficients of 10^{-5} to 10^{-6} molar solutions at 24 °C

Compound	λ_{max}/nm (log(ε/dm^3 mol^{-1} cm^{-1} 10^3)	
	THF solution	Water solution
H52	356 (4.71), 504 (4.35), 636 (4.46), 708 (4.59)	Not soluble
Co52[a]	355 (4.69), 455 (4.08), 643 (4.67)	Not soluble
Ni52	326 (4.65), 482 (4.26), 661 (4.62)	Not soluble
Cu52	352 (4.62), 496 (4.19), 664 (4.65)	Not soluble
Zn52	375 (4.81), 672 (4.84)	Not soluble
H73	357 (4.75), 501 (4.37), 634 (4.49), 704 (4.59)	335 (4.54), 508 (4.14), 623 (4.15)
Co73[a]	354 (4.69), 456 (4.09), 645 (4.68)	334 (4.53), 430 (4.09), 634 (4.41)
Ni73	327 (4.65), 483 (4.28), 661 (4.63)	320 (4.54), 486 (4.18), 623 (4.31)
Cu73	351 (4.63), 496 (4.20), 662 (4.66)	338 (4.57), 502 (4.19), 652 (4.38)
Zn73	372 (4.83), 668 (4.84)	364 (4.69), 661 (4.59)

[a]Fast decomposition occurs in THF solution under O_2 and light.

Table 4 Langmuir film formation and LB film formation[a] properties

Compound	Area per molecule/Å^2	Film collapse pressure/mN m^{-1}	Transfer ratio	Thickness of transferred monolayer/Å
H52	110	31	1.25	21 ± 0.3
Co52[a]	165	16[b]		
Ni52	150	32		
Cu52	110	16.5	*ca.* 2	23 ± 0.3
H73	—	—[c]		
Co73[a]	—	—[d]		
Ni73	155	17		
Cu73	150	37		

[a]Transferred onto silicon ⟨111⟩ wafer. [b]Collapse pressure was not well defined since the pressure constantly increased with decreasing area. [c]No obvious collapse pressure (1.0 mN m^{-1} at 1532 Å^2 and 15 mN m^{-1} at 112 Å^2). [d]No obvious collapse pressure (1.0 mN m^{-1} at 900 Å^2 and 15 mN m^{-1} at 45 Å^2).

the mesophase but we prefer to call it a solvent containing thermotropic mesophase rather than a lyotropic mesophase. In general, the thermotropic mesomorphism of amphitropic mesogens has been shown to be affected by small amounts of solvent[29] and opens interesting opportunities for the processing of these materials.

Langmuir–Blodgett (LB) films

Langmuir (L) films were prepared of all the samples except the zinc containing derivatives and the results are summarised in Table 4 and Fig. 4. Three different types of behaviour were observed: a) **H52**, **Ni52**, and **Cu73** formed stable films at the air–water interface with reversible isotherms and relatively high collapse pressures of >30 mN m^{-1}. b) **Co52**, **Cu52**, and **Ni73** also formed stable films but their collapse pressures were less well defined and of lower values (16–17 mN m^{-1}). Surface pressures were already built up at very low pressure values of 2–4 mN m^{-1} which is indicative of a strong intermolecular interaction even at large molecular areas. c) **H73**, and **Co73** did not form stable films and surface pressures already built up at very large molecular areas (*e. g.* $\pi = 2$ mN m^{-1} at $A = 1000$ Å^2 for **Co73**) and increased constantly with decreasing area. Representative isotherms of all three types of behaviour are shown in Fig. 4.

Molecular areas between 150 and 165 Å^2 found for **Co52**, **Ni52**, **Ni73**, and **Cu73** suggest a flat-on orientation of the macrocycle on the water surface with the side chains partially dissolved in the sub-phase (Fig. 5). This hypothesis is also supported by the invariance of the occupied molecular area in the L film to the different chain lengths. Smaller values of 110 Å^2 were measured for **H52** and **Cu52** which essentially is the molecular area of the macrocycle including the sulfur of the thioether groups. A flat-on orientation is therefore more likely than an edge-on orientation that would only cover 92 Å^2 taking a rather big inter-macrocycle (intra-columnar) distance of 4.5 Å.

Monolayer LB films of **H52**, **Cu52** and **Ni73** were prepared on hydrophilic substrates such as silicon ⟨111⟩ wafers and quartz slides. Attempts to transfer multilayers resulted in the desorption of the first layer. Drying of the first layer in vacuum over $CaCl_2$ prior to subsequent transfers did not result in any improvement. **H52** was transferred with a ratio of 1.25 and a film thickness of 21 Å was determined by X-ray reflectivity. The X-ray results reasonably agreed with the calculated electron density and revealed a low roughness of the LB film. **Cu52** was transferred with a high ratio of 2 that suggests major molecular rearrangements doubling the packing density in the monolayer with regard to the Langmuir film. A film thickness of 23 Å was determined by X-ray reflectivity. Monolayers of **Ni73** could be transferred onto hydrophilic substrates but the low quality of the LB films did not allow reliable X-ray measurements. The measured film thickness of 21–23 Å suggests an edge-on orientation of the macrocycle on the substrate and the transfer ratios of >1 support a change of packing order, *e.g.* the proposed reorientation from a flat-on to an edge-on packing (Fig. 5).

Both the type of metal ion and the chain length influence the self-assembling properties at the air–water interface of these materials. Longer ethylene oxide side chains do not improve the L film properties but rather worsen them (except for **Cu73**). Cobalt as central metal ion disturbs the self-assembling process, as was also found for the self-organisation process into mesophases, while copper and nickel ions can improve the self-assembling properties with regard to the metal-free macrocycle. However, the complexity of the behaviour and the limited number of compounds investigated make it difficult to reveal general trends.

A crucial dependence of the L and LB film behaviour on the central metal ion agrees with the findings of a detailed study on

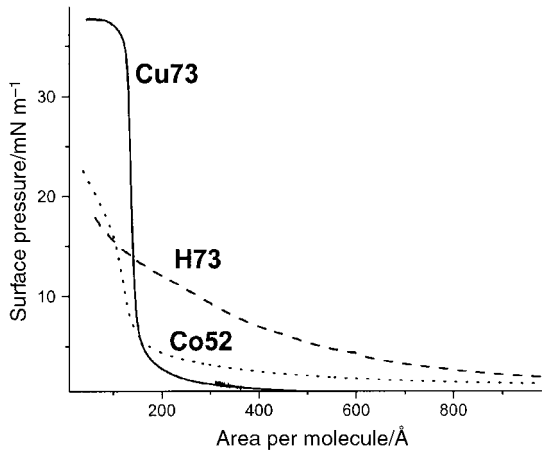

Fig. 4 Pressure–area isotherms of Langmuir films with defined collapse pressure (**Cu73**), ill-defined collapse pressure (**Co52**), and no obvious collapse pressure (**H73**).

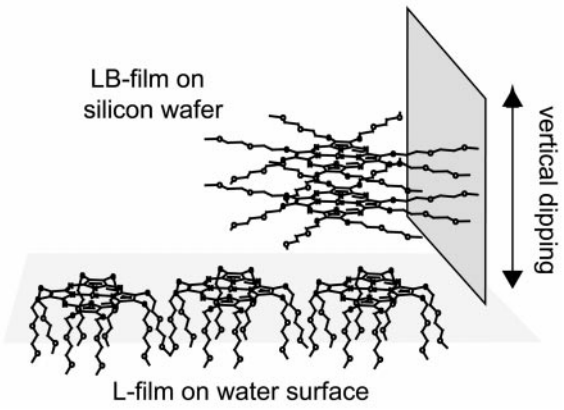

Fig. 5 Change from the face-on to the edge-on orientation of **Cu52** during the transfer from the L film to the LB film.

LB films of phthalocyanines.[30] The cobalt and zinc complexes were shown to axially coordinate water molecules in the L films that interrupt a close packing of the macrocycles, while the nickel derivative did not show any axial ligands. An intermediate behaviour was found for the L films of the copper complex. At low surface pressures the square planar Cu(II) seems to be ligated by water which, however, was expelled at higher surface pressures to allow the close face to face packing of the aromatic macrocycles. A similar trend was also reported for tetraphenylporphyrin derivatives where the nickel, cadmium, platinum and copper complexes showed good film-forming properties whereas the zinc and cobalt analogues did not.[31]

Spin-coating layers

Homogeneous multilayer films of **Cu52** (*ca.* 300 nm thick) on silica slides (UV/VIS measurements, 2×2 cm) or silicon wafer (X-ray reflectivity measurements, 2×1 cm) were prepared by spin-coating from THF solution ($10\%_{mass}$). The absorption spectra of the layers showed a red-shift of the two Q-bands if compared with the monomer spectrum in solution, whereas the absorption bands at around 500 nm and 350 nm were blue-shifted. Also, a decrease of the extinction of the Q-band at higher wavelengths (around 664 nm), relatively to the Q-band at lower wavelengths (around 620 nm), was found (Fig. 6).

Therefore, a columnar stacking of macrocycles comparable to the Col_{hd} mesophase of **Cu52** can be excluded, since this arrangement would cause a blue-shift of the Q-bands.[14, 32] However, a tilted columnar arrangement, where the molecular plane is not normal to the axis, has been shown to cause a red-shift and a decrease in the extinction coefficient of the Q-band. Tilted columnar arrangements are typical for the crystalline phases of porphyrazines and phthalocyanines and usually are of oblique or rectangular symmetry.[33] The films did not show dichroism by polarised UV/VIS spectroscopy, suggesting a random in-plane arrangement of micro-domains of the macrocycles. X-Ray reflectivity patterns of identically prepared films on silica wafer displayed a Bragg peak at $2\theta = 4.8°$, indicating a periodicity of horizontal layers at 30 °C. Beside this main peak a number of sharp peaks of lower intensity were found at wide angles ($2\theta > 20°$) revealing a crystalline morphology of the film (Fig. 7). The diffraction pattern therefore is in agreement with an expected crystalline phase of **Cu52** at room temperature, but the crystallinity obviously did not interfere with the formation of a layer structure parallel to the substrate. Calculation of the correlation length gave a value of 1846 Å, about the thickness of the film,[34] and the calculated thickness of each horizontal layer is 18.3 Å. This is slightly smaller than the intercolumnar distance in the Col_h phase of **Cu52** (20.5 Å) and therefore is consistent with a tilted columnar structure. Consequently, the spin-coated films presumably consist of well defined layers of tilted columnar

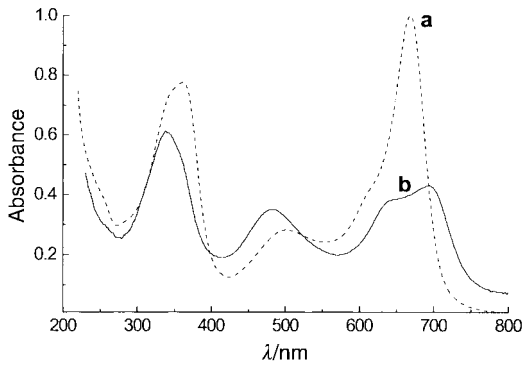

Fig. 6 UV/VIS spectra of **Cu52** in 10^{-6} mol L^{-1} THF solution (a) and as spin-coated film on silica slides (b) at 30 °C.

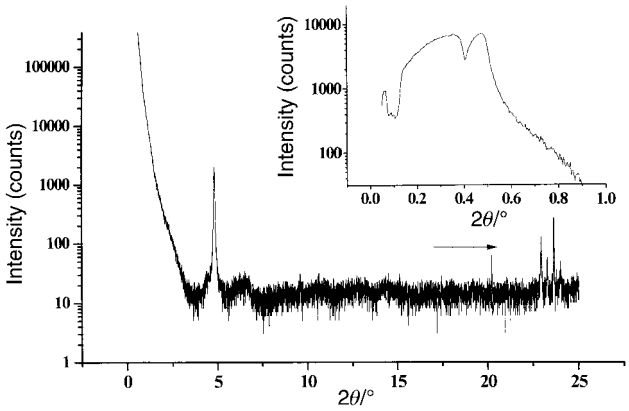

Fig. 7 X-Ray reflectivity data for the spin-coated film of **Cu52** on a silica wafer at 30 °C. The arrow marks wide angle diffraction peaks that are indicative of the crystalline state of the film.

stacks of macrocycles that arrange edge-on with regard to the substrate. The morphology is crystalline and the orientation of the columns within the plane of the layers is random on a microscopic scale.

Annealing of the films at 80 °C for 24 h resulted in a rearrangement of the molecules and an appearance of dichroism of all absorption bands between 350–700 nm. In addition, the intensity of the Q-band at 695 nm decreased and the maximum was blue-shifted to 680 nm, whereas the intensity of the Q-band at 650 nm increased. A bathochromic shift of 15 nm was found for the maximum at 480 nm. This process was reversible and the blue-shift is in agreement with the formation of a less tilted columnar arrangement of the macrocycles within the temperature range of the Col_h mesophase of **Cu52**. The appearance of a dichroism also pointed to an 'edge-on' orientation of the macrocycles, rather than a 'plane-on' orientation, relative to the substrate. However, the strength and the orientation of the dichroism was strongly depending on the thermal history of the sample and changing between different domains.

Identical annealing of the films on silica wafer did not change the X-ray reflectivity pattern at 30 °C which is in agreement with the reversible optical behaviour. Thus, the layer structure seems to be unaffected by the phase transitions into the mesophase and back to the crystalline state. The freshly spin-coated films obviously represented the thermodynamically preferred supramolecular structure. X-Ray reflectivity measurements within the temperature range of the mesophase were not possible due to limitations of the instrument.

Conclusions

We have shown that the mesomorphism of porphyrazines containing oligo(oxyethylene) side chains is generally similar to that of their alkyl chain substituted parents. However, a more careful choice of the metal ion is necessary in the case of oligoether chains, in order to obtain mesomorphism. Furthermore, it is possible to tune the mesomorphism (*e.g.* transition temperatures and mesophase orientation) of the amphiphilic discotic mesogen by adding polar or non-polar organic non-solvents. Homogeneous films of **Cu52** could be easily prepared by the spin-coating method, but an optically anisotropic behaviour was only found within the temperature range of the mesophase, whereas a horizontal layer structure of probably randomly arranged macrocycles, or small aggregates, was obtained at ambient temperatures. The processability of the amphiphilic compounds in L and LB films also strongly depended on the type of metal ion and the length of the oligo(oxyethylene) chain. **H52**, **Ni52** and **Cu73** showed the best L film properties. Only monolayer LB films could be

transferred on to silicon wafers while multiple dipping of the substrate resulted in a desorption of the first layer.

Acknowledgements

We thank the Volkswagen-Foundation (grant No I/65908), the University of Exeter and the NEDO International Collaboration Found for financial support. We are grateful to Professor Timothy M. Swager (Massachusetts Institute of Technology) for the use of his equipment and for discussion.

References

1 *Phthalocyanines, Properties and Applications*, eds. C. C. Leznoff and A. B. P. Lever, Vols. **1–4**, VCH, New York, 1989–1996, and references cited therein
2 N. B. McKeown, *Phthalocyanine Materials*, Cambridge University Press, Cambridge, 1998, and references therein; F. Bonosi, G. Ricciardi, F. Lelj and G. Martini, *J. Phys. Chem.*, 1993, **97**, 9181; P. Roisin, J. D. Wright, R. J. M. Nolte, O. E. Sielcken and S. C. Thorpe, *J. Mater. Chem.*, 1992, **2**, 131; R. H. Poynter, M. J. Cook, M. A. Chesters, D. A. Slater, J. McMurdo and K. Welford, *Thin Solid Films*, 1994, **243**, 346.
3 K. E. Treacher, G. J. Clarkson, Z. Ali-Adib and N. B. McKeown, *Chem Commun.*, 1996, 73.
4 J. M. Kroon, R. B. M. Koehorst, M. van Dijk, G. M. Sanders and E. J. R. Sudhölter, *J. Mater. Chem.*, 1997, **7**, 615; C. Piechocki and J. Simon, *New J. Chem.*, 1985, **9**, 159.
5 K. E. Treacher, G. J. Clarkson and N. B. McKeown, *Mol. Cryst. Liq. Cryst.*, 1995, **260**, 255; G. J. Clarkson, N. B. McKeown and K. E. Treacher, *J. Chem. Soc., Perkin Trans. 1*, 1995, 1817.
6 N. B. McKeown and J. Painter, *J. Mater. Chem.*, 1994, **4**, 1153.
7 N. Boden, R. J. Bushby, K. W. Jolley, M. C. Holmes and F. Sixl, *Mol. Cryst. Liq. Cryst.*, 1987, **152**, 37, and references cited therein.
8 N. Kobayashi, R. Higashi, K. Ishii, K. Hatsusaka and K. Ohta, *Bull. Chem. Soc. Jpn.*, 1999, **72**, 1263.
9 M. Kimura, T. Muto, H. Takimoto, K. Wada, K. Ohta, K. Hanabusa, H. Shirai and N. Kobayashi, *Langmuir*, 2000, **16**, 2078.
10 J. A. Hyatt, *J. Org. Chem.*, 1978, **43**, 1809.
11 C. F. van Nostrum and R. J. M. Nolte, *Chem. Commun.*, 1996, 2385 and references cited therein.
12 D. Markovitsi, J.-J. Andre, A. Mathis, J. Simon, P. Spegt, G. Weill and M. Ziliox, *Chem. Phys. Lett.*, 1984, **104**, 46.
13 F. Lelj, G. Morelli, G. Ricciardi, A. Roviello and A. Sirigu, *Liq. Cryst.*, 1992, 941; C. S. Velázques, G. A. Fox, W. E. Broderick, K. A. Andersen, O. P. Anderson, A. G. M. Barrett and B. M. Hoffman, *J. Am. Chem. Soc.*, 1992, **114**, 7416.
14 F. Bonosi, G. Ricciardi, F. Lelj and G. Martini, *J. Phys. Chem.*, 1993, **97**, 9181.
15 A. Davison and R. H. Holm, *Inorg. Synth.*, 1967, **10**, 8.
16 M. Lee and N-K. Oh, *J. Mater. Chem.*, 1996, **6**, 1079.
17 C. J. Schramm and B. M. Hoffman, *Inorg. Chem.*, 1980, **19**, 383.
18 H. Eichhorn, M. Rutloh, D. Wöhrle and J. Stumpe, *J. Chem. Soc., Perkin Trans. 2*, 1996, 1801.
19 J. Fitzgerald, W. Taylor and H. Owen, *Synthesis*, 1991, 686.
20 N. B. McKeown, *Phthalocyanine Materials*, Cambridge University Press, Cambridge, 1998, p. 78, Plate 2.
21 C. Destrade, P. Foucher, H. Gasparoux, Nguyen Huu Tinh, A. M. Levelut and J. Malthete, *Mol. Cryst. Liq. Cryst.*, 1984, **106**, 121.
22 Mg(II) tetraazaporphyrins **Mg52** and **Mg73** were also isolated and behaved similar to **Zn52** and **Zn73**. However, the magnesium derivatives were not further investigated due to great difficulties to obtain a purity of higher than 95%.
23 Slightly smaller intercolumnar distances were reported for a Co(II) octakis(octylthio)tetraazaporphyrazine when compared to the parent Cu(II), Ni(II), and Zn(II) complexes. However, the cobalt complex also displayed a Bragg peak at 5 Å indicating a higher intracolumnar packing order which was explained by the presence of larger amounts of Co(III) porphyrazin contamination. P. Doppelt and S. Huille, *New J. Chem.*, 1990, **14**, 607.
24 J. K. M. Sanders, N. Bampos, Z. Clyde-Watson, S. l. Darling, J. C. Hawley, Hee-Joon Kim, Chi Ching Mak and S. J. Webb, in *The Porphyrin Handbook*, ed. K. M. Kadish, K. M. Smith and R. Guilard, Academic Press, San Diego, 2000, vol. 3, and references therein; D. Wöhrle and G. Meyer, *Kontakte (Darmstadt)*, 1985, **3**, 38.
25 Single crystal structures of Fe(II), Mn(II), and Co(II) octakis(alkylthio)porphyrazines reveal axial sulfur metal coordination in the solid state. S. Belviso, G. Ricciardi and F. Lelj, *J. Mater. Chem.*, 2000, **10**, 297 and references therein. Also, the single crystal structure of the magnesium complex of a dithiacrown ether substituted tetraazaporphyrin contains one water molecule for each macrocycle so that the magnesium ions are axially linked to the crown ethers of adjacent azaporphyrins.C. F. van Nostrum, F. B. G. Benneker, H. Brussaard, H. Kooijman, N. Veldman, A. L. Spek, J. Schoonman, M. C. Feiters and R. J. M. Nolte, *Inorg. Chem.*, 1996, **35**, 959.
26 H. Eichhorn, M. Rutloh, J. Stumpe and D. Woehrle, *J. Chem. Soc., Perkin Trans. 2*, 1996, 1801; H. Eichhorn, *Synthese, thermotropes Verhalten und Photochemie mesogener sowie amorpher Porphyrazine*, Dissertation, Bremen, 1995
27 N. Kobayashi, R. Higashi, K. Ishii, K. Hatsusaka and K. Ohta, *Bull. Chem. Soc. Jpn.*, 1999, **72**, 1263; J. F. van der Pol, E. Neeleman, J. C. van Mittenburg, J. W. Zwikker, R. J. M. Nolte and W. Drenth, *Macromolecules*, 1990, **23**, 155; J. Vacus and J. Simon, *Adv. Mater.*, 1995, **7**, 797.
28 G. W. Gray and J. W. Goodby, *Smectic Liquid Crystals*, Leonard Hill, Glasgow and London, 1984.
29 B. Neumann, C. Sauer, S. Diele and C. Tschierske, *J. Mater. Chem.*, 1996, **6**, 1087; G. Lattermann, G. Staufer and G. Brezesinski, *Liq. Cryst.*, 1991, **10**, 169.
30 S. Fouriaux, F. Armand, O. Araspin, A. Ruaudel-Teixier, E. M. Maya, P. Vazquez and T. Torres, *J. Phys. Chem.*, 1996, **100**, 16984.
31 R. Bonnett, S. Ioannou, A. G. James, C. W. Pitt and M. M. Z. Soe, *J. Mater. Chem.*, 1993, **3**, 793.
32 W. J. Schutte, M. Sluyters-Rehbach and J. H. Sluyters, *J. Phys. Chem.*, 1993, **97**, 6069; M. Fujiki, H. Tabei and T. Kurihara, *J. Phys. Chem.*, 1988, **92**, 1281.
33 D. Wöhrle and G. Meyer, *Kontakte (Darmstadt)*, 1985, issue 3, 38
34 An exact calculation of the film thickness was not possible because of the missing Kiessig oscillations.